

Ligature-induced periodontitis promotes *Dnmt3a*^{R878H}-driven clonal hematopoiesis

Qiao Yuan,^{1*} Min Liao,^{2*} Ziyao Zhuang,^{1*} Chenyan Huang,¹ Rixin Chen,¹ Yuxian Song,¹ Yu Wu,¹ Peihui Zou,³ Lili Li,¹ Hua Nie,¹ Miaomiao Zhang,¹ Shiyuan Song,¹ Yanfen Li¹ and Fuhua Yan¹

¹Department of Periodontology, Nanjing Stomatological Hospital, Affiliated Hospital of Medical School, Institute of Stomatology, Nanjing University, Nanjing; ²TransThera Sciences (Nanjing), Inc, Nanjing and ³Department of Periodontology, Peking University School and Hospital of Stomatology, Peking University, Beijing, China

*QY, ML and ZZ contributed equally as first authors.

Correspondence: Y. Li

liyanfen2003@126.com

F. Yan

yanfh@nju.edu.cn

Received: July 28, 2025.

Accepted: December 30, 2025.

Early view: January 22, 2026.

<https://doi.org/10.3324/haematol.2025.288827>

©2026 Ferrata Storti Foundation

Published under a CC BY-NC license



Methods

***In Vivo* Micro-Computed Tomography (Micro-CT)**

Mice were anesthetized by inhalation of 2% isoflurane delivered in air and positioned for scanning. The maxillae were subsequently imaged using an *in vivo* micro-computed tomography (micro-CT) system (SkyScan 1172, Bruker). Scans were acquired at an isotropic voxel resolution of 18 μm . Projection images were reconstructed into cross-sectional slices using the manufacturer's software (DataViewer v1.5.6.2, Bruker). To quantify alveolar bone loss, the distance from the cemento-enamel junction (CEJ) to the alveolar bone crest (ABC) was measured on mesial, buccal, distal and palatal surfaces of the maxillary second molars within the reconstructed images using DataViewer software (version 1.5.4.0, Bruker, Germany).

Histological analysis of periodontal tissue

After being decalcified in 10% EDTA solution (pH 7.2) for 4 weeks, the maxillae were sectioned and stained with hematoxylin and eosin (H&E) or tartrate-resistant acid phosphatase (TRAP). The stained sections were scanned using a Panoramic MIDI II scanner (3DHISTECH).

Cells preparations and sample collection

During preparation of BM single-cell suspensions, mouse femurs were flushed with chilled HBSS⁺ buffer (Hank's balanced salt solution supplemented with 2% fetal bovine serum, 1% penicillin/streptomycin, and 1% HEPES). Cells were forced through a 70- μm nylon cell strainer to obtain single-cell suspensions for subsequent flow cytometric analysis and fluorescence-activated cell sorting (FACS). To collect BM extracellular fluid, femurs were rinsed with 500 μL ice-cold PBS (Gibco, Thermo Fisher Scientific), followed by centrifugation at 500 \times g for 5 minutes at 4°C to harvest supernatants.

Peripheral blood (PB) mature cells were lysed with ACK buffer (NH₄Cl 150 mM, KHCO₃ 10 mM, Na₂EDTA 0.1 mM, adjust the pH to 7.2–7.4), followed by staining for chimerism analysis using flow cytometry. Serum was collected via retro-orbital bleeding. Specifically, whole blood was allowed to clot undisturbed at room temperature for 30 minutes, centrifuged at 12000 \times g for 10 minutes at 4°C to remove clots, and the supernatant was subsequently harvested.

Gingival tissues around the area of ligature placement (and the contralateral control area) were dissected within 3 minutes post-euthanasia and digested with cold PBS (Gibco, Thermo Fisher Scientific) supplemented with 2% FBS (Gibco). Gingival tissues were then cut into 1-mm² pieces with scissor and digested in freshly prepared digestion medium consisting of 2 mg/ml collagenase type II (Yeasten) and 1 mg/ml DNase I (Yeasten). The digestion was performed at 37°C with orbital shaking at 200 rpm for 30 minutes and subsequently quenched by adding EDTA (Invitrogen, Thermo Fisher Scientific) to a final concentration of 5 mM. Single-cell suspensions were obtained by mechanically disrupting the tissues through a 70-µm nylon mesh using a syringe plunger, followed by filtration for subsequent staining for FACS analysis.

Flow cytometry and sorting

Flow cytometry analysis was performed on a Sony SA3800 flow cytometer (Sony) and analyzed using FlowJo™ software (Becton, Dickinson and Company). Cell sorting was conducted with the Sony SH800s internal sorter, with target populations sorted into HBSS⁺ buffer. Non-lysed BM cells were used for hematopoietic stem and progenitor cell (HSPC) analysis (antibodies included lineage-biotin cocktail, streptavidin APC-Cy™7, c-kit APC, Sca-1 PE/Cy7, CD150 PE, CD34 Alexa Fluor 700, CD16/32 FITC, and CD135 PE-CF594) and lineage analysis (antibodies targeting CD11b, Gr1, B220, and CD3). PB mature cell chimerism analysis included antibodies against CD11b, B220, CD3, CD45.1 and CD45.2. A detailed list of antibodies is provided in *Online Supplementary Information Table S1*.

Bone marrow transplantation

BM cells were isolated from *Dnmt3a*^{R878H/+}*Vav1-cre*⁺ mice (R878H, CD45.2) and *Dnmt3a*^{R878H/+}*Vav1-cre*⁻ littermates (WT, CD45.2), as well as congenic WT (CD45.1) mice. As shown in Figure 2A, in the experimental group, lethally irradiated (10 Gy) CD45.1/2 recipient mice received 1×10⁵ R878H or WT BM cells mixed with 5×10⁵ WT CD45.1 BM cells. 1 month after BM transplantation, 50% of R878H and WT recipient mice received LIP. Peripheral blood from recipients was analyzed monthly for donor-derived chimerism (myeloid cells, B cells and T cells). An antibody panel (CD3, B220, CD11b, CD45.1 and CD45.2) was used to assess peripheral blood chimerism.

UID mRNA-seq and data analysis

Gingival CD45.2⁺ and CD11b⁺ cells were isolated using the Sony SH800s internal cell sorter from R878H recipients and WT recipients. All procedures involving unique molecular identifier (UID) mRNA analysis, including library preparation and high-throughput sequencing of the sorted cells, were performed by Wuhan Kangce Technology Co., Ltd. Total RNA was extracted from the sorted cells using TRIzol® Reagent (Thermo Fisher, cat. no. 15596026) following the manufacturer's protocol. To eliminate genomic DNA contamination, extracted RNA samples were treated with DNase I (NEB, cat. no. M0303L). RNA purity was assessed by measuring A260/A280 ratios on a NanoDrop™ OneC spectrophotometer (Thermo Fisher), while RNA integrity was verified using the LabChip® GX Touch system (Revvity). Subsequently, RNA concentration was accurately quantified using a Qubit® 3.0 Fluorometer with the Qubit™ RNA Broad Range Assay Kit (Thermo Fisher, cat. no. Q10210). For RNA sequencing library construction, total RNA was processed with the KC™ Digital mRNA Library Prep Kit (Seqhealth Tech. Co., Ltd, Wuhan, China) according to the manufacturer's specifications. Final enriched libraries were quantified and subjected to paired-end 150-bp (PE150) sequencing on the DNBSEQ-T7 platform (MGI).

Cytokine antibody array

Serum samples were collected from recipient mice via retro-orbital venous plexus bleeding. Whole blood was clotted at room temperature for 30 min without disturbance, followed by centrifugation at 12,000 × g for 15 min at 4°C to remove coagulated material. The supernatant (serum) was collected, aliquoted into single-use vials, and stored at -80°C until analysis. Prior to detection, samples were subjected to 2-fold dilution and analyzed using a mouse antibody array kit (QAM-CAA-4000, RayBiotech). This glass chip-based platform simultaneously quantifies 200 cytokine proteins through immobilized antibody capture.

Quantitative real-time PCR

Total RNA was extracted from gingival cells using TRIzol® reagent (Invitrogen) following the manufacturer's instructions. RNA concentrations were normalized, and cDNA was synthesized using the PrimeScript™ RT Reagent Kit (Takara, Cat #

RR047A). The resulting cDNA was analyzed on a QuantStudio™ 3 Real-Time PCR System (Applied Biosystems) with PowerUp™ SYBR™ Green Master Mix (Applied Biosystems, Cat # A25780) and specified primers. For full primer sequences, refer to *Online Supplementary Table S2*.

Statistical analysis

After confirming normality, data were analyzed using a two-way ANOVA followed by Sidak's multiple comparisons test. All statistical analyses were performed with GraphPad Prism software (version 8; GraphPad Inc.). All data are shown as mean ± SEM. *P*-value <0.05 was considered statistically significant.

Supplemental Figures and Figure legends

Fig. S1

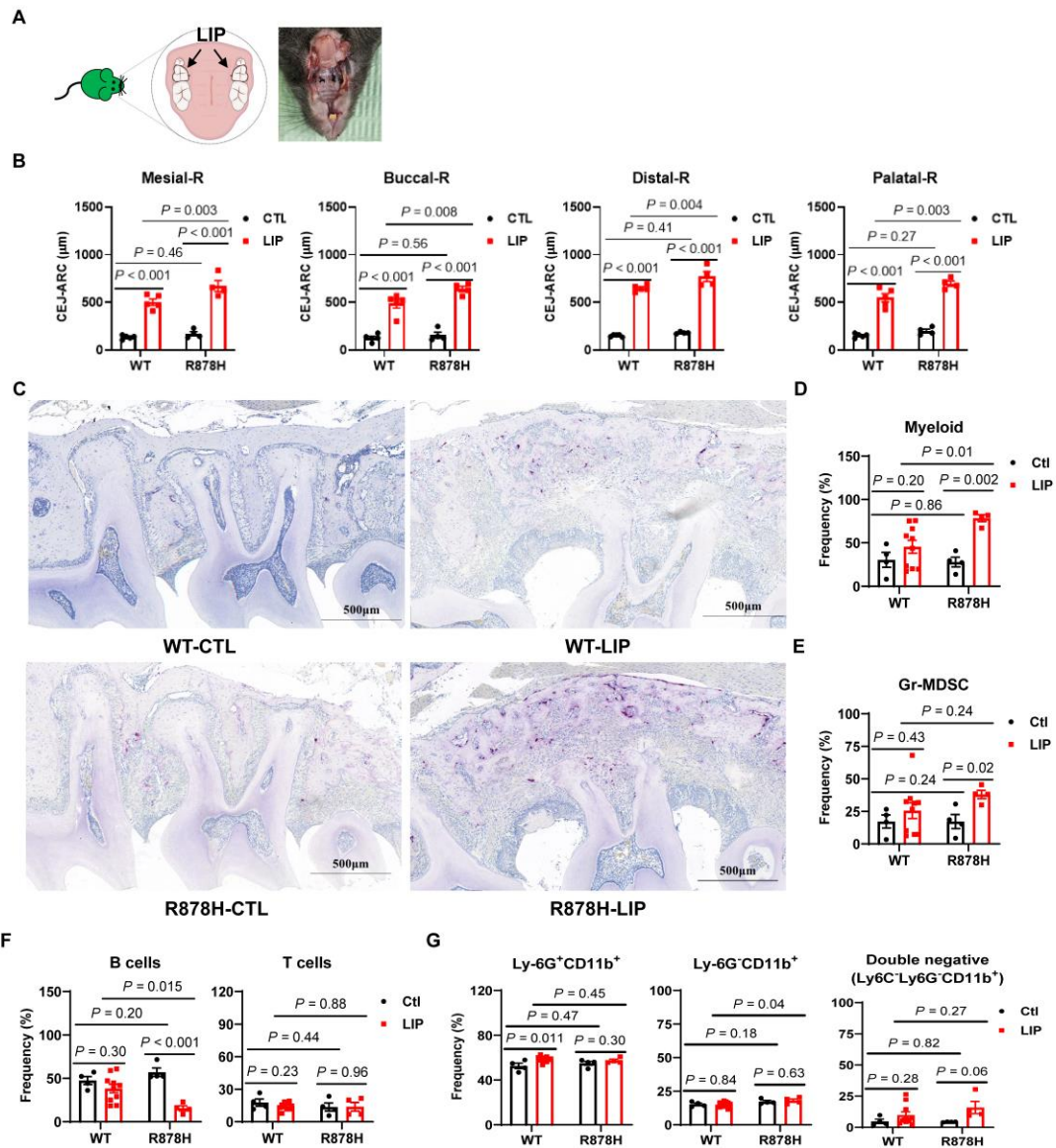


Figure S1 Dnmt3a R878H accelerates alveolar bone resorption and infiltration of gingival inflammatory cells

(A) Schematic diagram and image of LIP. (B) Site-specific CEJ-ABC measurements (mesial, buccal, distal, palatal) of maxillary right second molars across groups. (C) Quantification of osteoclasts by tartrate-resistant acid phosphatase (TRAP) staining around the maxillary second molar. (D-F) The frequency of cell population in gingival tissues: (D) myeloid cells (CD45⁺ CD11b⁺), (E) Gr-MDSC, (F) B cells and T cells, (G) The frequency of CD45⁺ Ly6G⁺ CD11b⁺ cells, CD45⁺ Ly6G⁻ CD11b⁺ cells and CD45⁺ Ly6G⁻ Ly6G⁻ CD11b⁺ cells in gingival tissues. $n = 4-5$ mice (2-3 months) per

group from two independent experiments. All data above are shown as mean \pm SEM and were analyzed using a two-way ANOVA followed by Sidak's multiple comparisons test.

Fig. S2

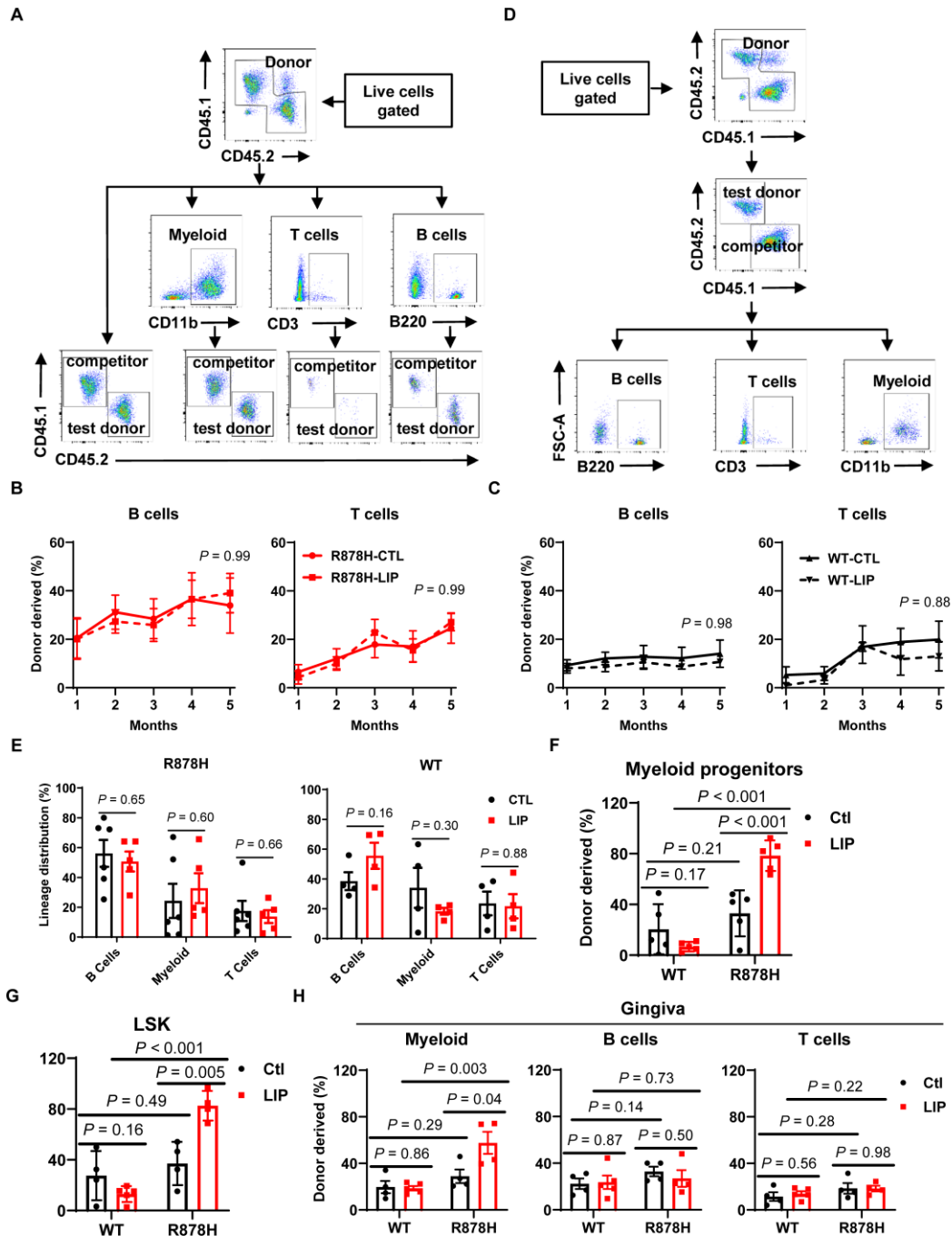


Figure S2 Ligature-induced periodontitis promotes Dnmt3a R878H-driven clonal hematopoiesis via a myeloid-biased phenotype

(A) Representative FACS plots identifying donor-derived (CD45.2⁺) contribution to myeloid cells (CD11b⁺), T cells (CD3⁺) cells and B cells (B220⁺) from R878H and WT mice. (B–C) Donor-derived (CD45.2⁺) contribution to B cells (B220⁺) and T cells (CD3⁺) from R878H (B) and WT (C) mice. (D) Representative FACS plots identifying lineage distribution to B cells (B220⁺), T cells (CD3⁺) cells and myeloid cells (CD11b⁺) in the bone marrow of recipients at the fifth month after transplantation. (E) Lineage distribution of B cells, myeloid cells and T cells among donor-derived cells in the PB of recipients carrying R878H or WT BM cells treated with or without LIP at the 5th month after transplantation. (F–G) The histograms show the percentage of myeloid progenitor cells (F) and LSK (G) in LIP group (red) and CTL group (black) in the bone marrow. (H) The percentage of R878H/WT-derived myeloid cells (CD11b⁺), B cells (B220⁺) and T cells (CD3⁺) within gingival tissue of indicated recipient mice. All data above are shown as mean \pm SEM and were analyzed using a two-way ANOVA followed by Sidak's multiple comparisons test.

Fig. S3

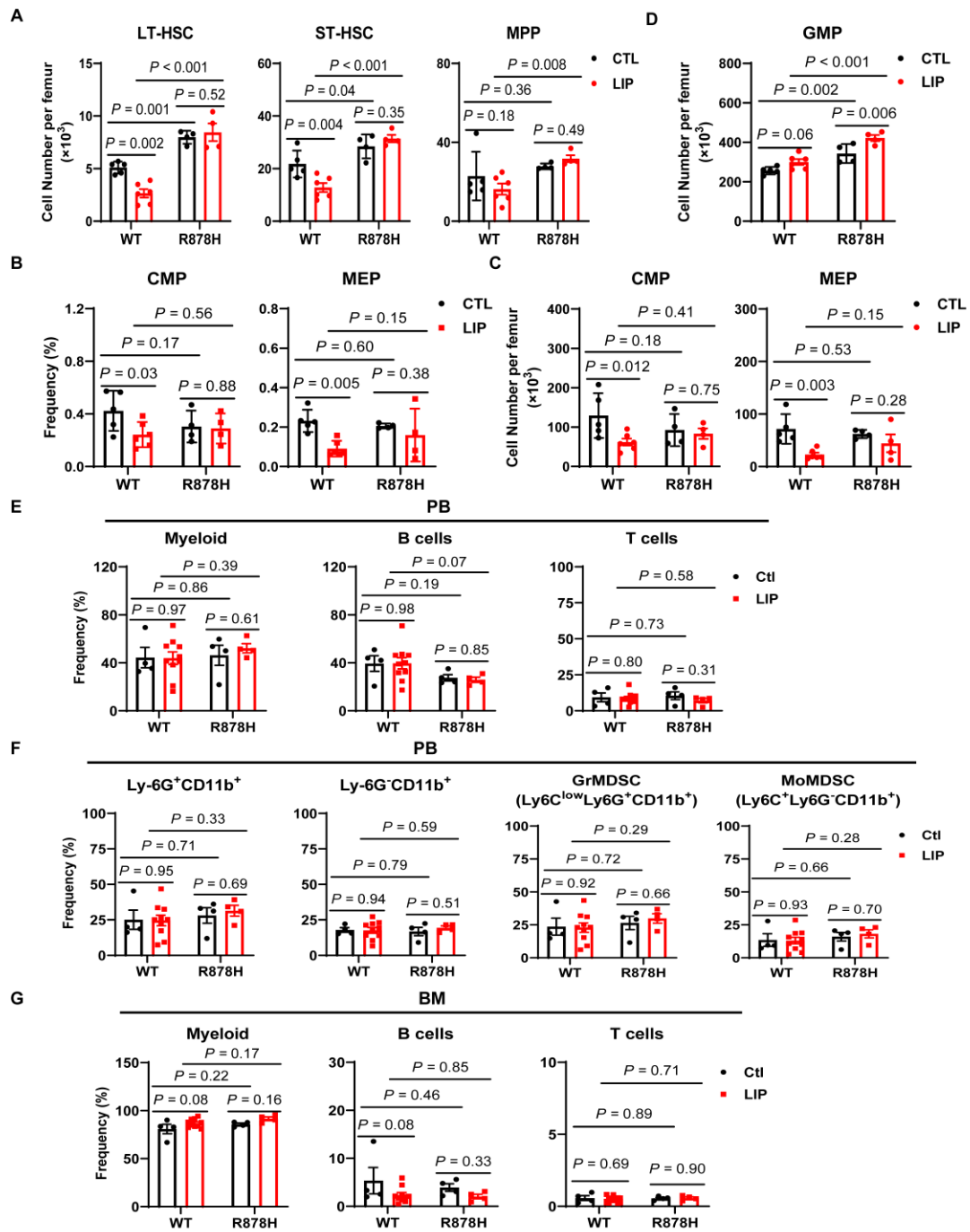


Figure S3 R878H HSCs exhibit greater resistance to inflammation induced by periodontitis than WT HSCs

(A) Histogram of absolute counts for BM populations: LT-HSCs, ST-HSCs and MPPs. (B–C) Histograms showing the frequency (B) and absolute count (C) of CMPs and MEPs in the bone marrow. (D) Histogram showing absolute counts of GMPs in bone

marrow. (E) The frequency of lineage cells (myeloid, B and T cells) in peripheral blood. (F) The frequency of Ly-6G⁺ CD11b⁺ cells, Ly-6G⁻ CD11b⁺ cells, Gr-MDSC (Ly6C^{low} Ly6G⁺ CD11b⁺) and Mo-MDSC (Ly6C⁺ Ly6G⁻ CD11b⁺) in the peripheral blood of WT and R878H mice treated with or without LIP. (G) Frequency of myeloid cells (CD11b⁺), B cells (B220⁺) and T cells (CD3⁺) of WT and R878H mice subjected or not (control) to LIP for 21 days in the BM. *n* = 4–5 mice per group from two independent experiments. All data above are shown as mean ± SEM and were analyzed using a two-way ANOVA followed by Sidak's multiple comparisons test.

Fig. S4

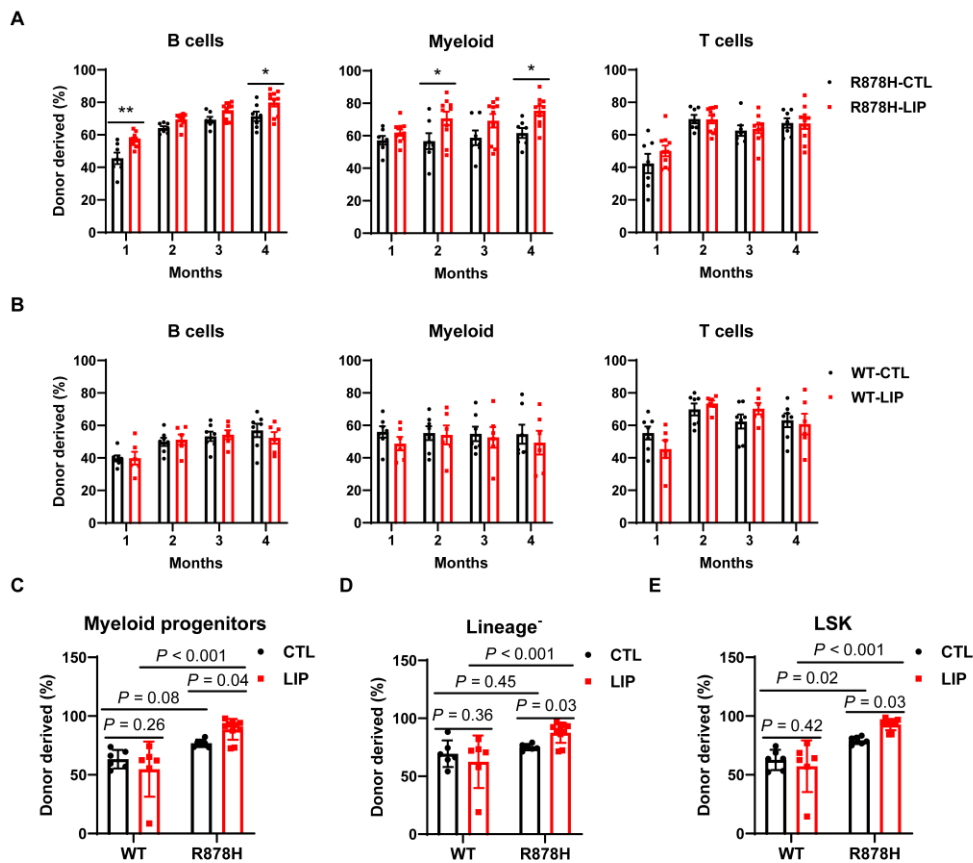


Figure S4 LIP-stressed R878H HSCs maintain a competitive advantage and a myeloid-biases differentiation

(A–B) Donor-derived (CD45.2⁺) contribution to B cells (B220⁺), myeloid cells (CD11b⁺) and T cells (CD3⁺) from R878H (A) and WT (B) recipient mice subjected, or not (control), to LIP. (C–E) The histograms show the percentage of WT/R878H-

derived myeloid progenitor cells (lineage⁻ Sca-1⁻ c-kit⁺) (C) lineage⁻ (D) and LSK (E) in LIP group (red) and CTL group (black). $n = 6-7$ mice per group from two independent experiments. All data above are shown as mean \pm SEM. * $P < 0.05$, ** $P < 0.01$. All data were analyzed using a two-way ANOVA followed by Sidak's multiple comparisons test.

Fig. S5

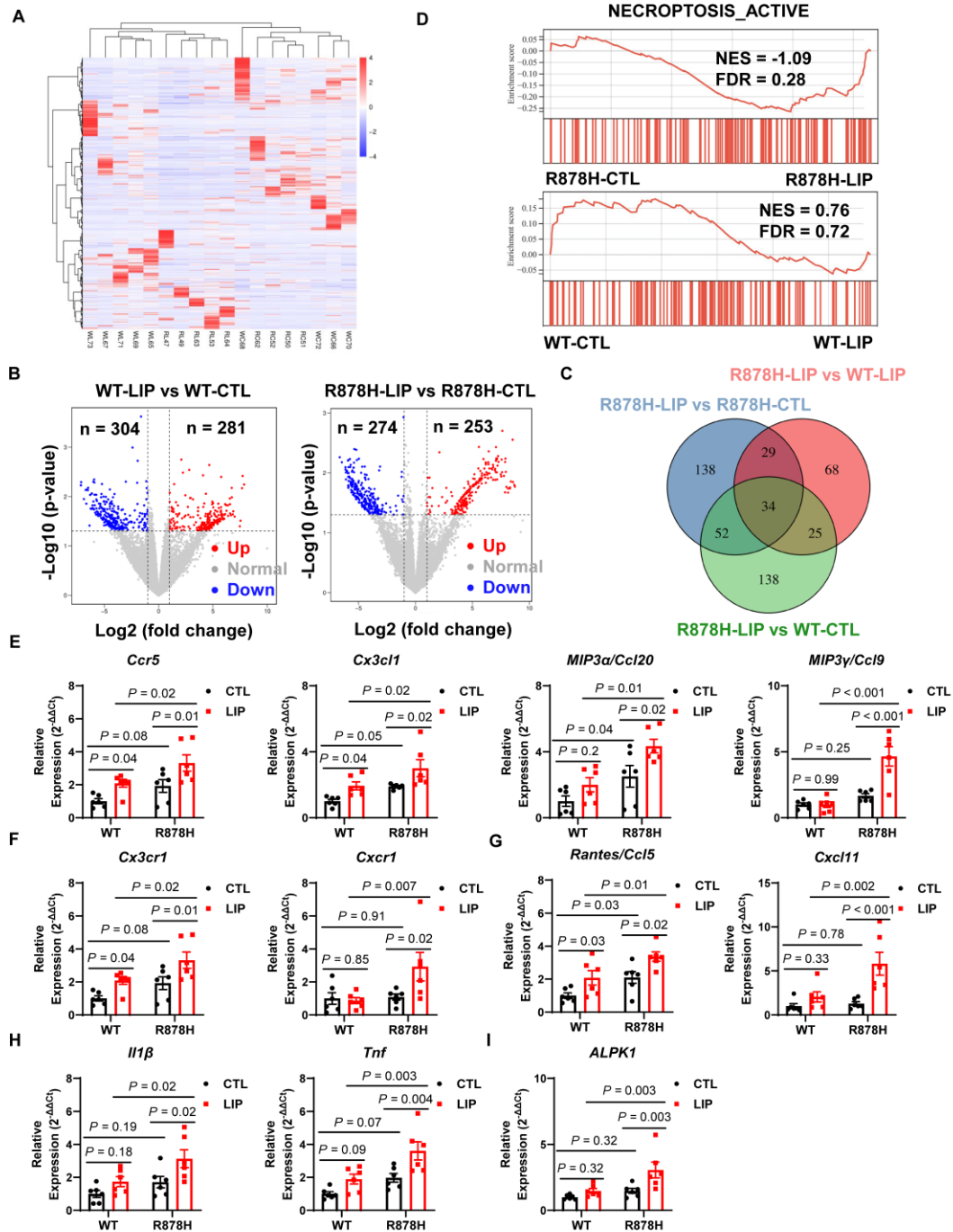


Figure S5 Activation of chemokine signaling in Dnmt3a R878H mutant myeloid

cells in gingiva under periodontitis

(A) The heatmap of differential expressed genes in each group. (B) All differentially expressed genes are shown in volcano plot. Highlighted genes in color (blue: downregulated, red: upregulated) are more than twofold differentially expressed ($P < 0.05$) in WT-LIP versus WT-CTL and R878H-LIP versus R878H-CTL groups. $n = 3$ independent mice per group. (C) The Venn diagram shows the upregulated genes in R878H-LIP group when compared to R878H-CTL group, WT-LIP group and WT-CTL group, respectively. (D) Gene set enrichment analysis (GSEA) of necroptosis activation-related genes in R878H and WT cells treated with LIP versus CTL. (E-I) Quantitative real-time PCR (qPCR) was performed to confirm the expression of some chemokine-related genes (*Ccr5*, *Cx3cl1*, *Ccl20*, *Ccl9*, *Cx3cr1*, *Cxcr1*, *Ccl5*, *Cxcl11*, *Il1 β* , *Tnf* and *Alpk1*) in the gingiva of recipient mice. All data above are shown as mean \pm SEM and were analyzed using a two-way ANOVA followed by Sidak's multiple comparisons test.

Fig. S6

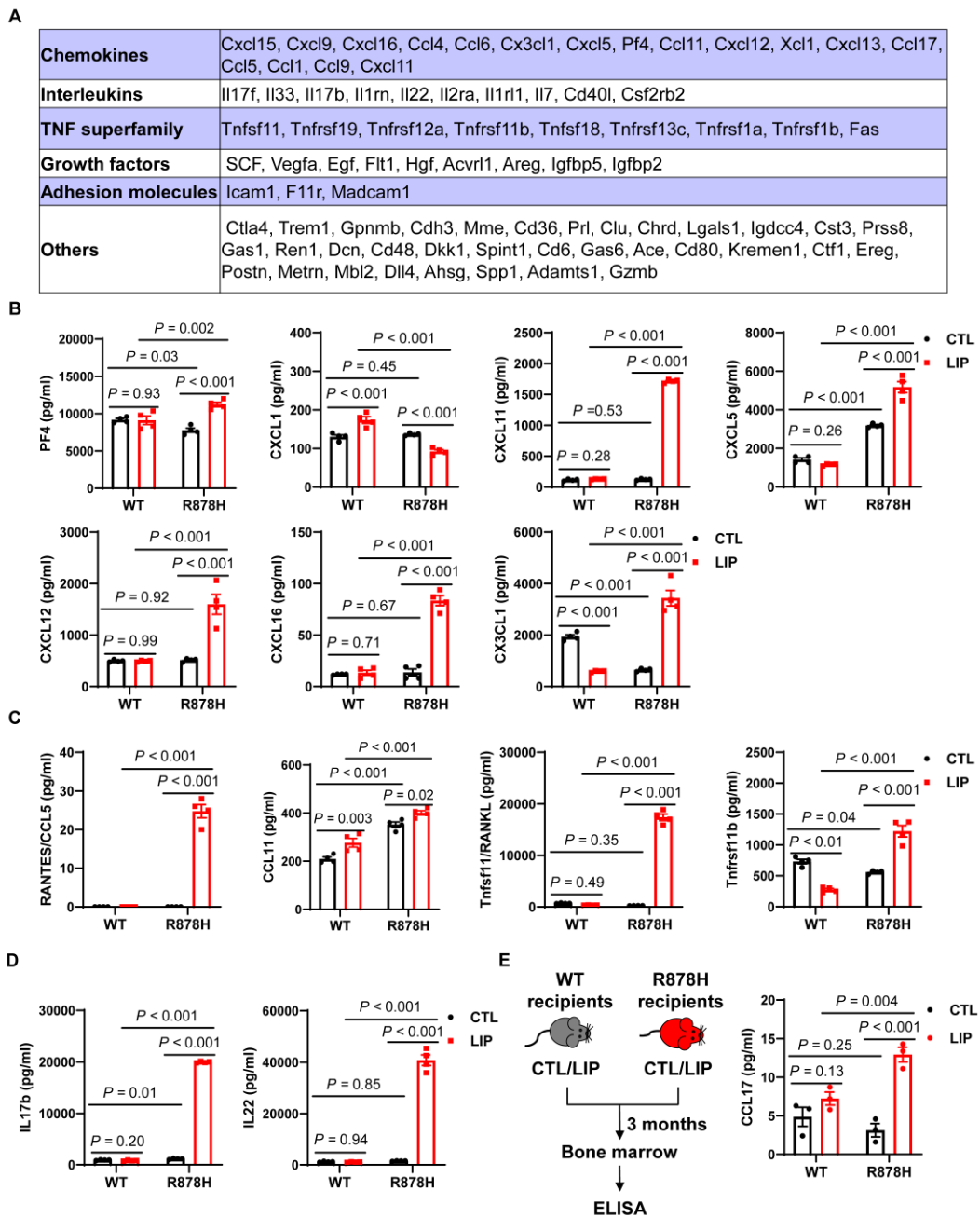


Figure S6 Dnmt3a R878H drives systemic chemokine storm in periodontitis associated clonal hematopoiesis

(A) The table depicts the proteins specifically upregulated in R878H-LIP group shown in the Venn diagram. (B–D) ELISA results show the level of chemokines (PF4, CXCL1, CXCL11, CXCL5, CXCL12, CXCL16, CX3CL1, CCL5, CCL11) and cytokines (RANKL, TNFRSF11b, IL17b, IL22) in the serum of recipient mice ($n = 4/\text{group}$). (E) ELISA was performed to confirm the level of CCL17 in the bone marrow of recipient

mice ($n = 3/\text{group}$). All data above are shown as mean \pm SEM and were analyzed using a two-way ANOVA followed by Sidak's multiple comparisons test.

Fig. S7

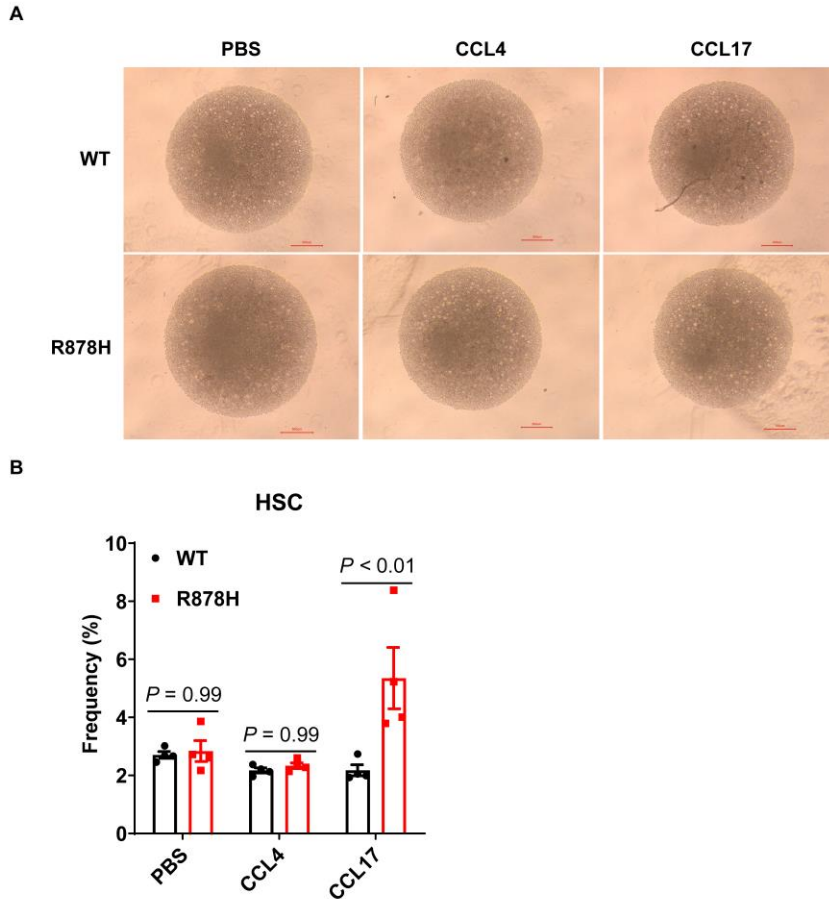


Figure S7 CCL17 expands R878H HSCs *in vitro*

(A–B) 400 HSCs ($\text{CD}48^- \text{CD}150^+ \text{LSK}$) were freshly isolated from either WT or R878H mice, and the HSCs were cultured *in vitro* in the presence or absence of CCL4/CCL17 (100 ng/mL) for 6 days (all HSCs were cultured in SFEM medium supplemented with 30 ng/mL SCF, 30 ng/mL TPO and 100 U/mL Penicillin–Streptomycin). (A) On the 6th day, cell growth was monitored by a light microscopy, and images were acquired under an inverted microscope (Olympus CKX41). Scale bar, 500 μm . (B) The frequency of HSCs ($\text{CD}150^+ \text{CD}48^- \text{c-KIT}^+ \text{SCA-1}^+$) was analyzed on days 6 ($n = 4$).

Table S1. KEY RESOURCES TABLE

REAGENT or RESOURCE	SOURCE	IDENTIFIER
Antibodies		
Biotin Ter-119 anti-mouse (clone TER-119)	Biolegend	Cat# 116204, RRID: AB_313705
Biotin CD3 ϵ anti-mouse (clone 145-2C11)	Biolegend	Cat# 100304, RRID: AB_312669
Biotin CD4 anti-mouse (clone RM4-5)	Biolegend	Cat# 100508, RRID: AB_312711
Biotin CD8a anti-mouse (clone 53-6.7)	Biolegend	Cat# 100704, RRID: AB_312743
Biotin CD11b anti-mouse (clone M1/70)	Biolegend	Cat# 101204, RRID: AB_312787
Biotin Ly-6G and Ly-6C anti-mouse (clone RB6-8C5)	Biolegend	Cat# 108404, RRID: AB_313369
Biotin B220 anti-mouse (clone RA3-6B2)	Biolegend	Cat# 103204, RRID: AB_312989
APC CD3 ϵ anti-mouse (clone 145-2C11)	Biolegend	Cat# 100312, RRID: AB_312677
Alexa Fluor® 700 Gr1 anti-mouse (clone RB6-8C5)	Biolegend	Cat# 108422, RRID: AB_2137487
PerCP-Cy TM 5.5 CD11b anti-mouse (clone M1/70)	Biolegend	Cat# 101228, RRID: AB_893232
Pacific Blue TM B220 anti-mouse (clone RA3-6B2)	Biolegend	Cat# 103227, RRID: AB_492876
PE CD45.1 anti-mouse (clone A20)	Biolegend	Cat# 110708, RRID: AB_313497
FITC CD45.2 anti-mouse (clone 104)	Biolegend	Cat# 109806, RRID: AB_313443

Streptavidin APC-eFluor780	Thermo Fisher Scientific	Cat# 47-4317-82, RRID: AB_10366688
APC CD117 anti-mouse (clone 2B8)	Thermo Fisher Scientific	Cat# 17-1171-83, RRID: AB_469431
PE-Cy™7 Sca-1 anti-mouse (clone D7)	Thermo Fisher Scientific	Cat# 25-5981-82, RRID: AB_469669
Alexa Fluor® 700 CD34 anti-mouse (clone RAM34)	Thermo Fisher Scientific	Cat# 56-0341-82, RRID: AB_493998
FITC CD34 anti-mouse (clone RAM34)	Thermo Fisher Scientific	Cat# 11-0341-85, RRID: AB_465022
PE-CF594 CD135 anti-mouse (clone A2F10.1)	BD Biosciences	Cat# 562537, RRID: AB_2737639
FITC CD16/CD32 anti-mouse (clone 2.4G2)	BD Biosciences	Cat# 553144, RRID: AB_394659
Chemicals, Peptides, and Recombinant Proteins		
Fetal Bovine Serum	GEMINI	900-108
DAPI	Sigma-Aldrich	D8417
Penicillin-Streptomycin	Gibco	15140122
D-Hanks	Solarbio	H1045
Hepes	Solarbio	H1095
PBS	Solarbio	P1022
KHCO ₃	Sigma-Aldrich	298-14-6
NH ₄ Cl	Sigma-Aldrich	A9434
EDTA	Sigma-Aldrich	E6758
TRIzol	Invitrogen	15596018
Critical Commercial Assays		
PrimeScript RT reagent Kit	Takara	Cat# RR047A
PowerUp™ SYBR™ Green mix	Applied Biosystems	Cat# A25780

Mouse Cytokine Array Q4000	Raybiotech	Cat# QAM-CAA-4000-1
DNase I	NEB	Cat#M0303L
Qubit™ RNA Broad Range Assay kit	Thermo Fisher	Cat# Q10210
Dispase II Dispersing enzyme II	Yeasen Biotechnology	Cat# 40104ES80
Collagenase II Collagenase type II	Yeasen Biotechnology	Cat# 40508ES76
Mouse CCL4/MIP-1β ELISA	Multisciences Biotech	Cat# EK262
Mouse CCL22/MDC ELISA Kit	Multisciences Biotech	Cat# EK2216
Human CCL17/TARC ELISA Kit	Multisciences Biotech	Cat# EK1115
Mouse CCL5/RANTES ELISA Kit	Multisciences Biotech	Cat# EK2129
Human CX3CL1/Fractalkine	Multisciences Biotech	Cat# EK1209
Mouse CCL11/Eotaxin ELISA Kit	Multisciences Biotech	Cat# EK2130
Mouse CXCL16 ELISA Kit	Multisciences Biotech	Cat# EK2254
Mouse CXCL1/KC ELISA Kit	Multisciences Biotech	Cat# EK296
Mouse TRANCE/TNFSF11/RANKL ELISA	Multisciences Biotech	Cat# EK2208
Mouse IL-22 ELISA Kit	Multisciences Biotech	Cat# EK222
Mouse IL-17B ELISA Kit	Invitrogen	Cat# EMIL17B
Mouse OPG (TNFRSF11B) ELISA Kit	Invitrogen	Cat# EMTNFRSF11B
Mouse I-TAC/CXCL11 ELISA Kit	Invitrogen	Cat# EMCXCL11
Mouse PF4 ELISA Kit	Invitrogen	Cat# EEL120
Mouse SDF-1 alpha/CXCL12 ELISA Kit	Invitrogen	Cat# EMCXCL12

Mouse LIX/CXCL5 ELISA Kit	Invitrogen	Cat# EMCXCL5
7-AAD reactive staining solution	Thermo Fisher	Cat# 00-6993-50
Xylene	Shhushi	Cat#1002341922
Anhydrous ethanol	Shhushi	Cat#100092680
Yihong dye solution	Yormbio	Cat#YM1002
Hematoxylin dye solution	Yormbio	Cat#YM1001
Hematoxylin differentiation solution	Yormbio	Cat#YM1013
Neutral gum	Sinopharm Chemical	Cat#10004160
Tartrate-Resistant Acid Phosphatase(TRAP) Stain Kit	Solarbio	Cat#G1492
Experimental Models: Organisms/Strains		
Mouse: <i>Dnmt3a</i> ^{flox-R878H/+}	(Liao M, 2022)	N/A
Mouse: B6.Cg- <i>Commd10</i> ^{Tg(Vav1-icre)A2Kio/J}	Jackson Laboratory	Stock# 008610
Mouse: B6.SJL- <i>Ptprc</i> ^a <i>Pepc</i> ^b /BoyJ	Jackson Laboratory	Stock# 002014
Oligonucleotides		
Primers for mouse genotyping and qRT-PCR, see Table S2	Synthesized at TsingKe Biological Technology	N/A
Software and Algorithms		
GraphPad Prism 6	GraphPad Software	N/A
FlowJo™ Software	Becton, Dickinson and Company	N/A
Adobe Photoshop CS6	Adobe	N/A

Adobe Illustrator CC 2018	Adobe	N/A
---------------------------	-------	-----

Table S2 Differentially expressed genes (Top 30 upregulated genes)

R878H-LIP v.s R878H-CTL			
GeneName	logCPM	logFC	PValue
Krt78	5.01	9.10	0.00008
Krt6a	4.45	8.55	0.00050
Mir6236	5.14	5.60	0.00164
Nr4a3	5.67	2.96	0.00206
Abca12	3.23	8.77	0.00357
Nfe2l3	2.94	8.44	0.00441
Gm26760	2.63	8.16	0.00537
Ccl22	2.15	7.62	0.00537
Tns4	1.93	7.40	0.00599
Foxf1	1.54	6.81	0.00611
Csflr	6.06	1.57	0.00612
Wmp	1.87	7.35	0.00625
5430437J10Rik	4.57	6.40	0.00634
Rnf170-ps	2.59	6.68	0.00707
Arsi	1.35	6.61	0.00746
4933402D24Rik	1.60	7.03	0.00778
2200002D01Rik	7.52	2.50	0.00779
Klrb1a	1.28	6.66	0.00860
Dcstamp	1.08	6.30	0.00922
Gm32006	4.05	4.95	0.00964
Gm29170	1.26	6.69	0.00975
Tacstd2	3.48	5.52	0.01005
Rtn2	2.57	5.16	0.01018

Psca	1.23	6.56	0.01032
Hmgb1-rs16	0.84	5.90	0.01068
Tmsb10	6.37	1.72	0.01069
Ccl4	1.76	5.70	0.01078
Klri2	1.86	6.00	0.01126
Tstd1	2.88	5.76	0.01167
Npc2	5.72	1.76	0.01172
R878H-LIP v.s WT-LIP			
GeneName	logCPM	logFC	PValue
Gsdmc2	3.00	7.78	0.00184
Cftr	1.96	6.60	0.00254
Gm49066	1.96	6.51	0.00521
Gm56667	2.69	6.34	0.00544
Gm57349	2.74	5.13	0.00584
Mgat4c	1.88	6.48	0.00605
Spaca7b	2.48	7.23	0.00640
Gm7609	2.37	7.08	0.00653
Gm42648	2.18	6.88	0.00674
Rnf43	3.87	3.16	0.00677
Gm26592	1.73	6.37	0.00721
Gm52950	1.85	6.41	0.00796
ENSMUSG00000121342	1.85	6.41	0.00796
Impg2	3.15	4.02	0.00803
Gm13162	1.65	5.94	0.00810
Muc3	2.31	5.92	0.00827
Adamts19	1.74	6.06	0.00878
Scn11a	2.89	7.71	0.00922
Phgr1	3.36	5.04	0.00925
Zg16	2.23	5.70	0.00939

A430027C01Rik	3.03	7.85	0.00963
Igkv3-12	3.21	8.02	0.00972
Ighv2-9-1	1.26	5.36	0.00997
Gm20492	0.98	4.79	0.01009
9130213A22Rik	0.98	4.79	0.01009
Il22ra2	1.36	5.50	0.01014
Gm38266	1.03	5.21	0.01144
P2rx2	3.02	7.86	0.01155
Gm12708	1.06	4.95	0.01231
Gm42421	1.07	4.97	0.01236
R878H-LIP v.s WT-CTL			
GeneName	logCPM	logFC	PValue
Qdpr	6.61	1.44	0.00182
Ccl22	3.60	6.05	0.00269
Gsdmc2	3.11	8.03	0.00286
Khk	6.44	1.36	0.00376
Xist	3.78	4.19	0.00436
F8a	3.07	7.90	0.00493
Cd209c	1.85	6.54	0.00508
Retn	2.52	6.10	0.00527
Gm34643	2.44	7.16	0.00534
Gm33732	3.04	7.87	0.00567
Mlx	6.05	1.19	0.00626
Gm37653	3.03	6.69	0.00647
Gm10522	1.83	6.41	0.00647
Babam1	5.73	1.35	0.00663
Chrna9	2.59	7.39	0.00720
Tstd1	1.76	5.33	0.00727
Phgr1	3.46	5.81	0.00766

Igkv3-4	2.73	7.59	0.00857
Gm13162	1.69	6.22	0.00885
Gm42648	2.24	7.13	0.00901
Gm48583	1.67	6.41	0.00907
Fcgbp	3.88	4.79	0.00918
Cidea	2.70	4.74	0.00948
H2-Q10	8.45	1.13	0.00949
Spaca7b	2.56	7.48	0.00953
Htr7	1.27	5.62	0.00975
Gm34189	1.23	5.53	0.00976
4930414N06Rik	2.53	4.90	0.01077
Wmp	1.79	6.64	0.01124
Gm18807	1.55	6.11	0.01142

Table S3 Cytokine array results

(pg/ml)	WT-CTL-PB	WT-LIP-PB	R878H-CTL-PB	R878H-LIP-PB	LOD	MAX
AR	0.0	10.6	3.2	30.5	3.0	2,000.0
Axl	882.3	402.4	685.2	918.0	8.4	10,000.0
CD27L	31.6	26.0	18.2	5.2	22.0	6,666.7
CD30	54.1	54.9	38.6	50.2	9.0	10,000.0
CD40	3.8	11.7	7.5	7.4	3.0	1,111.1
CXCL16	16.3	59.1	82.6	88.2	0.3	1,000.0
EGF	1,524.2	387.9	136.6	2,075.1	0.9	2,000.0
E-selectin	4,938.7	4,250.5	5,648.4	5,450.9	2.6	4,000.0
Fractalkine	3,865.7	1,445.6	1,562.4	5,497.0	14.7	100,000.0
GITR	7.6	2.3	4.9	5.3	2.1	4,000.0
HGF	1,207.3	1,803.5	2,969.0	6,168.8	83.8	20,000.0
IGFBP-2	23,022.1	21,449.1	24,211.3	31,418.6	135.8	100,000.0
IGFBP-3	14,020.8	15,576.3	15,527.6	15,044.4	23.0	20,000.0
IGFBP-5	1,236.4	1,202.1	1,582.3	9,378.7	28.0	13,333.3
IGFBP-6	17,983.8	28,350.9	24,158.8	30,036.2	23.6	40,000.0
IGF-1	8,407.9	9,961.4	9,301.2	8,271.8	2.1	10,000.0
IL-12p70	0.0	9.2	0.0	5.0	5.7	4,000.0
IL-17E	101.6	125.8	93.0	53.8	26.9	40,000.0

IL-17F	0.0	41.4	0.0	143.7	107.4	40,000.0
IL-1ra	66.6	147.2	139.0	1,520.8	11.1	4,000.0
IL-2 Ra	560.3	570.1	584.7	1,445.9	10.2	10,000.0
IL-20	56.2	15.4	63.2	45.5	40.4	20,000.0
IL-23	0.0	49.9	0.0	0.0	44.1	4,444.4
IL-28	0.9	1.0	8.1	0.0	2.6	2,000.0
I-TAC	0.0	0.0	0.0	1,627.9	28.4	20,000.0
MDC	83.3	76.3	92.0	83.2	0.6	1,000.0
MIP-2	2.4	3.2	1.0	0.8	0.6	1,000.0
MIP-3a	101.4	41.7	40.6	74.9	0.8	1,000.0
OPN	13,713.1	16,188.6	17,512.9	20,612.0	36.8	20,000.0
OPG	527.3	212.7	422.8	815.2	8.3	2,222.2
Prolactin	374.0	557.1	403.8	2,531.8	8.5	1,111.1
Pro-MMP-9	44,380.6	54,553.1	57,234.7	40,887.6	16.6	100,000.0
P-selectin	2,951.1	3,353.2	2,784.1	2,970.9	8.2	1,333.3
Resistin	570.4	486.1	545.8	308.2	2.5	666.7
SCF	4.2	45.0	75.0	3,029.1	17.3	10,000.0
SDF-1a	759.8	770.0	805.7	1,118.2	42.1	100,000.0
THPO	55.6	386.3	235.4	160.3	153.4	33,333.3
VCAM-1	4,253.7	4,303.7	4,474.4	3,991.5	2.6	4,000.0
VEGF	48.3	105.1	61.8	564.8	4.4	4,000.0
VEGF-D	0.0	2.8	1.1	0.8	1.2	4,000.0
4-1BB	2,168.3	1,895.7	2,402.8	2,297.8	129.8	25,000.0
ACE	121,981.5	109,048.1	139,910.3	202,897.0	161.5	100,000.0
ALK-1	103.6	58.8	81.2	1,865.7	9.0	10,000.0
CT-1	75.5	0.0	77.1	104.2	38.7	40,000.0
CD27	0.0	56.7	0.0	0.0	20.0	25,000.0
CD40L	2,724.0	2,817.6	3,114.1	36,923.4	19.6	40,000.0
CTLA4	5.1	6.2	8.9	250.4	0.3	2,500.0
Decorin	2,929.3	4,861.3	3,425.2	7,797.1	1.1	5,000.0
Dkk-1	11,188.3	10,879.4	10,125.1	22,840.0	19.9	40,000.0
Dtk	33.9	20.0	76.9	41.3	4.9	20,000.0
Endoglin	478.0	392.8	462.1	504.5	6.4	10,000.0
Fcg RIIB	1,722.7	1,593.4	1,774.7	2,006.3	0.9	10,000.0
Flt-3L	788.2	816.2	749.7	901.9	0.8	25,000.0
Galectin-1	2,159.1	4,680.4	3,320.2	14,003.0	6.5	10,000.0
Galectin-3	623.0	649.8	669.9	741.6	0.4	2,000.0
Gas 1	774.9	775.7	768.2	1,918.3	1.7	2,000.0
Gas 6	2,138.0	2,335.8	2,418.3	3,658.7	0.5	2,500.0
GITR L	57.8	35.2	52.3	123.9	0.4	1,000.0
HAI-1	48.2	68.8	76.9	149.2	9.1	10,000.0
HGF R	177.0	527.7	131.1	244.9	20.4	25,000.0
IL-1 R4	714.4	655.8	528.2	823.3	11.3	40,000.0

IL-3 Rb	1,322.8	2,192.5	2,846.4	3,615.4	76.1	40,000.0
IL-9	50.4	92.2	49.4	49.7	3.0	20,000.0
JAM-A	2,798.8	2,445.1	2,519.5	5,290.2	2.3	5,000.0
Leptin R	238.5	314.7	301.9	301.5	6.4	5,000.0
L-Selectin	9,088.7	8,793.7	8,054.0	9,319.3	1.1	10,000.0
Lymphotactin	938.8	1,018.9	1,853.6	1,312.9	67.3	200,000.0
MadCAM-1	216.4	198.7	249.9	332.1	0.6	1,111.1
MFG-E8	144.8	393.9	198.7	351.4	2.6	13,333.3
MIP-3b	0.0	0.0	0.0	0.0	0.6	1,000.0
Neprilysin	649.0	632.3	857.2	6,988.9	15.0	20,000.0
Pentraxin 3	6,692.1	9,323.2	6,366.6	7,834.5	8.3	10,000.0
RAGE	4.9	33.9	15.1	2.7	8.6	25,000.0
TACI	203.2	240.7	302.4	309.5	9.5	50,000.0
TREM-1	125.2	173.6	157.9	2,731.1	7.7	10,000.0
TROY	63.2	93.6	48.2	886.9	6.2	4,000.0
TSLP	0.6	5.4	3.1	2.0	0.4	4,000.0
TWEAK R	22,668.4	31,101.7	27,038.6	72,055.6	10.9	25,000.0
VEGF R1	768.1	1,039.8	1,049.5	11,118.5	12.4	10,000.0
VEGF R3	107.8	142.3	128.8	156.8	7.2	10,000.0
bFGF	0.0	0.0	0.0	0.0	2.8	5,000.0
BLC	0.0	0.0	0.0	92.2	28.3	10,000.0
CD30L	0.0	0.0	0.0	0.0	0.9	2,000.0
Eotaxin	157.9	215.7	274.9	382.3	0.4	1,000.0
Eotaxin-2	0.0	0.0	0.0	0.0	2.6	1,000.0
Fas L	0.0	0.0	0.0	0.0	14.8	10,000.0
G-CSF	738.5	365.0	1,242.0	1,143.3	40.0	20,000.0
GM-CSF	0.0	0.0	0.0	0.0	5.4	10,000.0
ICAM-1	1,640.5	1,198.3	116.7	4,074.3	14.1	10,000.0
IFNg	0.0	0.0	0.0	0.0	12.0	4,000.0
IL-1a	8.9	0.0	0.0	4.0	1.2	2,000.0
IL-1b	0.0	0.0	0.0	0.0	7.9	4,000.0
IL-2	0.0	0.0	0.0	0.0	4.6	10,000.0
IL-3	4.5	0.7	6.6	0.0	0.3	2,000.0
IL-4	0.0	0.0	0.0	0.0	0.6	166.7
IL-5	0.0	0.0	0.0	0.0	27.3	10,000.0
IL-6	0.0	0.0	0.0	0.0	6.3	1,333.3
IL-7	0.0	0.0	0.0	70.6	12.4	1,111.1
IL-10	0.0	0.0	0.0	0.0	24.7	10,000.0
IL-12p40	0.0	0.0	0.0	0.0	5.5	1,000.0
IL-13	0.0	0.0	0.0	0.0	15.0	20,000.0
IL-15	0.0	0.0	0.0	0.0	47.5	100,000.0
IL-17	0.0	0.0	0.0	0.0	1.1	4,000.0
IL-21	2,922.8	1,900.5	2,726.3	1,720.2	56.5	20,000.0

KC	119.7	164.7	127.5	106.7	0.5	2,000.0
Leptin	1,610.4	2,833.4	6,859.7	0.0	57.1	100,000.0
LIX	1,301.0	1,070.8	3,061.2	2,749.4	13.2	20,000.0
MCP-1	0.0	0.0	0.0	0.0	3.4	4,000.0
MCP-5	23.4	5.2	3.5	0.0	0.6	1,000.0
MCSF	0.0	0.0	25.8	0.0	1.1	2,000.0
MIG	0.0	39.9	0.0	677.1	13.2	10,000.0
MIP-1a	0.0	0.0	0.0	0.0	2.1	10,000.0
MIP-1g	871.9	845.9	938.7	1,217.7	0.7	1,000.0
PF4	8,105.8	8,225.4	6,944.8	9,747.3	7.1	20,000.0
RANTES	0.0	0.0	0.0	26.9	1.2	4,000.0
TARC	0.0	6.8	0.0	34.6	1.6	4,000.0
TCA-3	0.0	0.0	0.0	10.6	0.9	2,000.0
TNF RI	208.1	225.4	212.6	299.0	0.2	500.0
TNF RII	672.7	694.7	700.4	930.3	0.6	2,000.0
TNFa	0.0	0.0	0.0	0.0	3.2	1,000.0
6Ckine	142.8	1.1	19.2	65.2	31.5	20,000.0
Activin A	9.7	1.7	13.7	3.6	2.1	4,000.0
ADAMTS1	549.6	341.0	360.6	10,682.6	26.2	13,333.3
Adiponectin	6,062.9	5,314.8	6,933.7	5,939.8	11.8	3,333.3
ANG-3	409.9	110.0	518.7	375.0	24.4	40,000.0
ANGPTL3	15,004.4	15,263.3	22,171.7	16,533.9	63.4	100,000.0
Artemin	20.8	0.4	14.5	8.8	0.9	4,000.0
CCL28	312.6	0.0	0.0	0.0	64.9	100,000.0
CD36	7,671.8	7,749.3	11,999.4	91,913.7	199.6	200,000.0
Chordin	771.3	303.8	412.9	2,248.6	10.9	3,333.3
CRP	3,600.1	3,008.2	4,150.1	3,750.1	6.4	4,000.0
E-Cadherin	2,120.7	1,710.5	2,157.1	1,857.3	2.5	10,000.0
Epigen	630.2	426.4	726.3	582.6	24.0	20,000.0
Epiregulin	2,603.2	790.5	2,630.6	3,487.2	205.4	200,000.0
Fas	104.0	45.6	128.7	215.9	16.3	10,000.0
Galectin-7	733.3	485.7	742.8	158.2	110.6	100,000.0
gp130	2,857.4	1,329.2	3,728.2	3,316.6	24.9	10,000.0
Granzyme B	435.0	243.9	294.4	6,656.0	16.4	6,666.7
Gremlin	1,550.0	265.5	1,287.2	819.2	79.6	100,000.0
IFNg R1	6.5	0.7	2.1	0.0	3.1	2,000.0
IL-17B	586.3	198.5	1,005.1	20,646.8	142.1	200,000.0
IL-17B R	12.4	117.1	1,270.8	227.6	201.2	100,000.0
IL-22	1,185.6	826.2	1,479.1	12,585.8	70.7	13,333.3
MIP-1b	28.4	3.5	9.6	10.4	1.3	4,000.0
MMP-2	11,992.9	10,984.3	19,578.6	18,775.5	28.8	20,000.0
MMP-3	8,033.2	6,784.4	7,989.0	7,830.7	3.8	10,000.0
MMP-10	12.5	2.6	7.8	8.5	0.4	1,000.0

PDGF-AA	892.5	726.1	1,081.1	800.1	1.6	1,333.3
Persephin	11.1	8.1	10.4	8.1	0.6	4,000.0
sFRP-3	93.7	5.9	69.7	56.2	5.2	20,000.0
Shh-N	12.6	0.0	2.1	0.0	5.6	3,333.3
SLAM	78.0	378.0	141.0	348.4	70.1	100,000.0
TCK-1	93,009.0	83,874.3	123,806.8	85,798.8	42.5	200,000.0
TECK	365.9	301.9	171.0	62.2	59.9	200,000.0
TGFb1	1,414.0	1,265.5	2,282.6	1,382.2	71.2	100,000.0
TRANCE	1,770.8	718.6	631.1	17,859.5	78.2	40,000.0
TremL1	13,327.3	11,076.1	14,703.2	11,542.6	32.6	13,333.3
TWEAK	164.6	130.6	250.1	121.4	29.1	20,000.0
VEGF-B	23.0	0.0	0.0	0.0	24.7	10,000.0
VEGF R2	58.6	6.3	8.3	26.8	4.4	3,333.3
B7-1	3,384.8	3,903.9	3,360.3	4,793.2	7.4	4,000.0
BAFF R	387.1	342.4	323.8	531.1	2.4	1,000.0
BTC	51.3	41.4	58.1	64.6	2.3	2,000.0
C5a	720.0	807.6	786.3	805.4	0.8	1,000.0
CCL6	566.4	1,184.6	711.9	721.4	9.4	40,000.0
CD48	2,164.5	2,573.9	2,130.4	4,822.9	2.2	2,000.0
CD6	36.5	64.9	48.6	81.1	1.0	1,000.0
Chemerin	69,365.5	88,639.5	74,607.8	72,839.5	106.3	100,000.0
Clusterin	7,640.1	7,710.5	7,444.3	45,235.9	85.3	100,000.0
Lungkine	0.0	50.3	0.0	879.7	277.1	200,000.0
Cystatin C	1,481.3	1,687.7	1,537.6	4,554.0	3.2	666.7
DAN	1,528.4	1,649.6	1,516.9	1,667.4	13.5	100,000.0
DLL4	958.2	2,131.4	2,595.0	3,115.0	145.0	40,000.0
EDAR	5,778.5	6,684.6	6,671.0	6,585.0	21.1	20,000.0
Endocan	5,596.6	5,551.5	6,018.2	6,086.0	13.1	20,000.0
Fetuin A	134,823.0	133,527.2	131,583.7	157,207.9	190.4	100,000.0
H60	124.9	88.4	127.6	139.7	3.1	2,000.0
IL-33	15.7	9.9	16.9	1,398.0	1.5	4,000.0
IL-7 Ra	14,490.4	9,562.5	12,973.4	14,758.3	90.6	40,000.0
Kremen-1	191.3	229.2	249.0	342.1	10.4	4,000.0
Limitin	122.1	78.4	105.2	112.2	2.4	1,000.0
Lipocalin-2	54,198.4	61,774.3	53,124.7	42,456.1	6.3	100,000.0
LOX-1	382.9	866.7	1,091.9	1,237.8	14.4	4,000.0
Marapsin	1.5	90.1	102.9	0.0	37.5	20,000.0
MBL-2	4,602.0	5,192.6	4,962.1	6,058.8	0.9	2,000.0
Meteorin	0.0	153.3	186.0	244.2	26.3	40,000.0
Nope	3,754.7	4,779.6	4,908.4	19,822.0	19.5	10,000.0
NOV	6,602.4	7,458.6	7,598.5	7,196.5	8.1	40,000.0
Osteoactivin	619.5	1,287.4	747.4	8,271.2	17.6	10,000.0
OX40 Ligand	1,028.7	1,273.7	1,020.8	1,044.3	4.8	4,000.0

P-Cadherin	633.7	863.6	552.2	5,728.4	8.6	4,000.0
Periostin	20,331.4	18,181.3	19,756.3	26,047.7	8.7	4,000.0
PlGF-2	149.7	122.2	147.7	149.6	1.0	1,000.0
Progranulin	49,559.4	26,607.8	51,087.9	30,610.2	23.6	100,000.0
Prostasin	18,356.6	20,444.7	17,711.0	48,397.6	34.9	100,000.0
Renin 1	41,238.9	45,746.1	40,759.8	94,485.0	80.1	40,000.0
Testican 3	2,771.0	2,393.5	2,803.9	3,139.5	18.8	40,000.0
TIM-1	13,494.8	16,059.8	12,709.6	14,734.0	102.8	100,000.0
TRAIL	0.0	94.6	51.6	64.9	12.6	10,000.0
Tryptase e	9,523.5	11,167.4	11,117.5	11,516.4	36.6	100,000.0